β-decay rate of ^{59}Fe in shell burning environment and its influence on the production of ^{60}Fe in a massive star

K. A. Li (李阔昂),[1,*] Y. H. Lam (蓝乙华),[1,†] C. Qi (亓冲),[2,‡] X. D. Tang (唐晓东),[1] and N. T. Zhang (张宁涛)[1]

[1]*Institute of Modern Physics, Chinese Academy of Sciences, Lanzhou 730000, China*
[2]*Department of Physics, Royal Institute of Technology, Stockholm, Sweden*

We deduced the stellar β-decay rate of ^{59}Fe at typical carbon-shell burning temperature by taking the experimental Gamow-Teller transition strengths of the ^{59}Fe excited states. The result is also compared with those derived from large-scale shell model calculations. The new rate is up to a factor of 2.5 lower than the theoretical rate of Fuller, Fowler, and Newman (FFN) and up to a factor of 5 higher than decay rate of Langanke and Martínez-Pinedo (LMP) in the temperature region $0.5 \leqslant T \leqslant 2$ GK. We estimated the impact of the newly determined rate on the synthesis of cosmic γ emitter ^{60}Fe in C-shell burning and explosive C/Ne burning using a one-zone model calculation. Our results show that ^{59}Fe stellar β decay plays an important role in ^{60}Fe nucleosynthesis, even though the uncertainty of the decay rate is rather large due to the error of B(GT) strengths.

I. INTRODUCTION

The radioactive isotope ^{60}Fe ($T_{1/2} = 2.62$ Myr) is an important nucleus for γ-ray astronomy. It is believed to be synthesized during hydrostatic burning in massive stars and explosive shell burning when stars end their life as a core collapse supernova. Due to its long lifetime, it can survive the end of stellar life, and is dispersed into the interstellar medium after explosion, and is further enriched by the next generation of stellar evolution. In similar stellar environments, the other long-lived isotope, ^{26}Al ($T_{1/2} = 0.717$ Myr), is thought to be coproduced. Their decay γ-ray fluxes reflect the averaged contributions of their production over the entire stellar evolution and over stellar groups with many individual sources, allowing for interpretation in terms of stellar and supernova burning sites, structure, and dynamics [1].

Usually the ratio of their fluxes is measured to avoid the uncertainty in the observation (e.g., the distance of γ-ray source) since they are produced in similar sites [2]. Observations by satellites RHESSI and INTEGRAL report ratios of the fluxes from the decays of ^{60}Fe to that of ^{26}Al are 0.17 ± 0.13 and 0.148 ± 0.060, respectively [2,3]. Both measurements are quite consistent with the early predicted value by Timmes *et al.* [4]. However, later calculations using improved stellar and nuclear physics yield larger ^{60}Fe/^{26}Al flux ratios. For instance, Woosley and Heger [5] predicted a flux ratio of ^{60}Fe /^{26}Al $= 0.45$, which is about a factor of 3 higher than the observation. Due to the uncertainties arising from both nuclear physics and the stellar model, it is challenging to identify where the problems come from, and a rather large ambiguity exists in the current prediction. To resolve this puzzle, it is essential to examine the crucial nuclear physics inputs and reduce their incurred uncertainties.

^{60}Fe is produced in massive stars during helium (He) shell burning ($T \sim 0.4$ GK) and carbon (C) shell burning ($T \sim 1.2$ GK), together with explosive carbon/neon (C/Ne) burning (peak temperature $T \sim 2.2$ GK) [1]. The main reaction flow is ^{58}Fe$(n,\gamma)^{59}$Fe$(n,\gamma)^{60}$Fe. Since ^{59}Fe is unstable ($T_{1/2} = 44.5$ days), ^{59}Fe$(n,\gamma)^{60}$Fe must compete with the β-decay of ^{59}Fe to produce an appreciable amount of ^{60}Fe. The survival possibility of ^{60}Fe also depends on its neutron capture and β-decay rates. As presented in reference [1], more than half of ^{60}Fe is synthesized during C-shell burning and explosive burning, where the temperature is higher than 1 GK. At such high temperature, the low-lying excited states of ^{59}Fe can be thermally populated with fractions sensitive to the environmental temperature. Even though most of these states decay by γ transition in the laboratory, the high temperature in stellar environments hinders this possibility and, as a result, weak interaction process becomes dominant. Owing to the favorable selection rule and higher decay energy, the stellar β-decay rate including the excited state contributions becomes much faster than its terrestrial rate.

In this paper, using the Gamow-Teller (GT) transition probability B(GT) values obtained from charge exchange reaction and the empirical $\log ft$ value of the β-decay process, we provide a new stellar β-decay rate for ^{59}Fe. The result is also compared with those derived from large-scale shell model calculations. The impact of the new rate on the production of ^{60}Fe is investigated with a one-zone model for C-shell burning and explosive C/Ne burning.

II. PREVIOUS WORKS ON THE ^{59}Fe DECAY IN STELLAR ENVIRONMENT

Fuller, Fowler, and Newman (FFN) systematically estimated the weak interaction rates of nuclei in the mass range $21 \leqslant A \leqslant 60$ with temperature range $0.01 \leqslant T \leqslant 100$ GK and density range $10 \leqslant \rho Y_e \leqslant 10^{11}$ g/cm^3 [6]. Four different weak interaction processes, including electron capture, positron capture, β^+ decay, and β^- decay, were considered in their calculation. Excitation energies and spins of each involved state were taken from the 1978 compilations [7]. To estimate the transition strengths of these states, experimentally

---

*Corresponding author: lika@impcas.ac.cn

†Corresponding author: lamyihua@gmail.com

‡Corresponding author: chongq@kth.se

determined transition matrix elements were employed, wherever available. The unmeasured allowed GT transition has been assigned an empirical value ($\log ft = 5$) unless there is an indication of $\log ft \gg 5$ despite satisfaction of the selection rule for an allowed transition. The independent particle model was employed to calculate GT resonances. The FFN weak interaction rates have been extensively used in early stellar simulations including the work by Timmes [4].

Takahashi and Yokoi studied the stellar decay rates of the *s*-process relevant nuclei [8]. The calculations were performed with a compilation of nuclear structure data that is more recent than that of FFN. A new decay process, which is bound-state β decay, was included. However, as their studies were focused on the main *s* process happening in asymptotic giant branch (AGB) stars, the maximum temperature did not exceed 0.5 GK, which is much lower than the typical temperature ($T > 1$ GK) of C/Ne-shell burnings crucial to the production of ^{60}Fe.

Langanke and Martínez-Pinedo (LMP) used a large-scale shell-model calculation to obtain electron capture and β-decay rates in the stellar environment. The LMP data set was based on a modified KB3 effective Hamiltonian developed from a realistic nucleon-nucleon interaction with optimization in the monopole interaction channel [9,10]. With more recent experimental data, the B(GT) resonances in the mass range $45 \leqslant A \leqslant 65$ are better described globally for its application in the same temperature and density range than FFN. In such stellar environments relevant to the ^{60}Fe nucleosynthesis, the difference of the ^{59}Fe β-decay rate between FFN and LMP is rather large. For example, at $T = 1.2$ GK (a typical C-shell burning temperature), the FFN rate is about ten times the LMP rate. Comparing with the FFN rate, the LMP rate focuses on the contribution from GT resonances. However, its predictive power on the B(GT) values of low-lying discrete states, which is crucial to stellar decay at high temperature and in a low density environment, might be overlooked [11].

III. CALCULATION OF THE β DECAY RATE OF ^{59}Fe IN STELLAR ENVIRONMENT

In the stellar environment, the nucleus is thermally populated to its excited states. The probability of its population in a particular state with excitation energy E_i and spin J_i is given by the following equation:

$$P_i = \frac{(2J_i + 1)e^{-\frac{E_i}{kT}}}{\sum_l (2J_l + 1)e^{-\frac{E_k}{kT}}}, \tag{1}$$

where k is the Boltzman constant and T is temperature. Due to the thermal population, the excited states of ^{59}Fe reach equilibrium by γ emission and photon absorption. These states can only decay by weak interaction. The stellar decay half-life $t(T)$ can be calculated using

$$\frac{1}{t(T)} = \sum_i \frac{P_i(T)}{t_i}. \tag{2}$$

Here t_i is the β decay half-life of the ith state of ^{59}Fe.

The stellar β-decay scheme of ^{59}Fe is shown in Fig. 1. Only allowed transitions are listed. Since the direct measurement of t_i is not feasible for most excitation states in the laboratory,
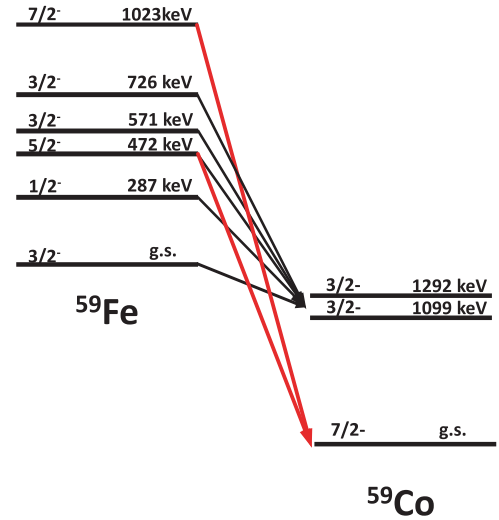

FIG. 1. The stellar β decay of ^{59}Fe. The red lines represent the allowed transitions to the ground state of ^{59}Co while the black lines indicate the allowed transition to the excited states of ^{59}Co.

three kinds of information (charge exchange reaction, empirical $\log ft$ distribution, and shell model calculation) are used to calculate the t_i.

In the present work, the fiducial stellar decay rate is calculated using the experimental transition strength for the crucial ^{59}Fe(472 keV) to ^{59}Co(g.s.) transition taken from charge exchange reactions, and using empirical $\log ft$ distributions for all the other allowed transitions. We include the ground state (g.s.) and the excited states of ^{59}Fe with excitation energies up to 1.02 MeV, which are shown in Fig. 1. As we will discuss in this section later, the states with higher excitation energy do not significantly contribute at $T < 2$ GK. In the NNDC database [12] the state 571 keV was tentatively assigned as $5/2^-$ according to an earlier fusion-evaporation measurement [13], leading to an allowed transition to the ground state of ^{59}Co. However, the analysis of γ transitions alone could not exclude the assignment of $3/2^-$ for this state. Furthermore, the J^π of the state 571 keV is identified as $3/2^-$ based on the analysis of angular distribution of differential cross section in experiments on ^{58}Fe(d,p) and ^{57}Fe(t,p) [14]. In this case, the β decay of this state will not be important because it cannot undergo an allowed transition to the ^{59}Co ground state. In addition, there are two states at 613 and 643 keV which are only weakly populated in two measurements, namely, ^{58}Fe(n,γ) [15] and ^{58}Fe(d,p) [16]. Important information such as J^π is missing. Therefore the two states at 613 and 643 keV are excluded in the fiducial stellar decay rate calculation because of missing J^π.

We also calculate the stellar decay rate with shell model calculations within the fp-shell space (including the $f_{7/2}$, $p_{3/2}$, $p_{1/2}$, and $f_{5/2}$ orbitals) by using the latest GXPF1a [17] and GXPF1j [18] effective interactions, to be compared with the LMP rate based on earlier shell model calculations. The experimental and theoretical level schemes of ^{59}Fe are shown in Fig. 2, where an overall good agreement is obtained. The results for both variants of GXPF1 interactions are quite
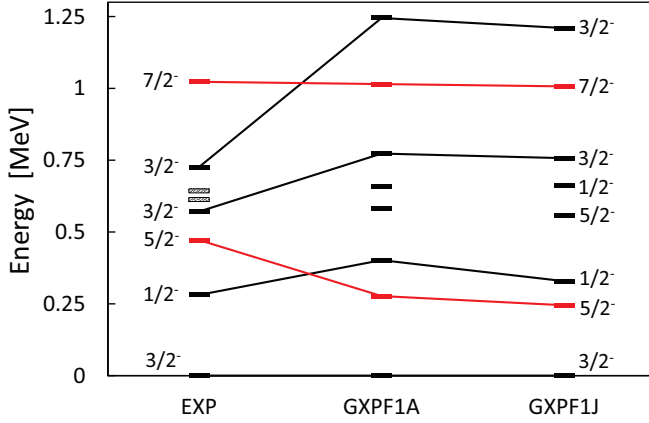
FIG. 2. The experimental and shell model energy levels up to 1 MeV of ^{59}Fe. The two dubious states (613 and 642 keV) excluded in the present work are shown with shaded marks.

similar to each other. Both calculations slightly underestimated the excitation energies for the first $5/2^-$ state. The lowest two $3/2^-$ excited states are calculated to be around 750 and 1250 keV, respectively. Excellent agreement between theory and experiment is also obtained for the low-lying states of ^{59}Co. The excitation energies of the first two $3/2^-$ states are calculated to be 1.087 and 1.167 MeV, respectively. Our shell model calculation provides B(GT) for the allowed transitions of the excited states, which dominate the decay rate for the ^{59}Fe in stellar environments. The contribution of the two states at 613 and 643 keV to the stellar decay rate is also discussed by tentatively assigning J^π based on the shell model calculation.

A. Transition strengths from the ^{59}Fe excited states to ^{59}Co

The most probable decay channel is determined by the transition mode and the β-decay energy. The allowed transitions to the ground state of ^{59}Co could significantly contribute to the decay rate due to their large decay energy. While the terrestrial β-decay rate of ^{59}Fe has been well studied in the laboratory, with a half-life of 44.495(9) days, the measurement of β decay of excited states is not feasible in the laboratory due to the fact that the γ transition is much faster than the β-decay process. The shell model calculation can be used to estimate the GT strength, even though there is still room for improvement in its precision.

To achieve a reliable estimation of the decay rate, indirect methods have been developed. Charge exchange reactions, such as ^{59}Co$(n, p)^{59}$Fe and ^{59}Co$(t, ^3$He$)^{59}$Fe, offer an indirect approach to determine the allowed transition strength for the ^{59}Co ground state to the excitation states of ^{59}Fe. Using the detailed balanced principle, the experimental B(GT)$_{ji}$ obtained from ^{59}Co(n, p) for the transition, ^{59}Co$(j)^{59}$Fe(i), is converted into the B(GT)$_{ij}$ of its inverse process, ^{59}Fe$(i)^{59}$Co(j), with

$$B(\text{GT})_{ij} = \frac{(2J_i + 1)B(\text{GT})_{ji}}{2J_j + 1},$$

where i and j are given states of ^{59}Fe and ^{59}Co, respectively. At present, only the ^{59}Co$(n, p)^{59}$Fe reaction has been studied, and

TABLE I. Summary of the experimental/emperical B(GT) and $\log ft$ values for the transitions from ^{59}Fe to ^{59}Co.

Transitions	B(GT)	$\log ft$
[a]472 keV → g.s.	$3.49(138) \times 10^{-2}$	$5.04^{-0.14}_{+0.22}$
[a]1023 keV → g.s.	$3.90(149) \times 10^{-3}$	$6.00^{-0.14}_{+0.21}$
[b]g.s. → 1099 keV	7.78×10^{-4}	6.70
[b]g.s. → 1292 keV	4.05×10^{-3}	5.98
[c]Other transitions in Fig. 1	4.87×10^{-3}	5.9

[a]Determined by the ^{59}Co$(n, p)^{59}$Fe reaction [20].
[b]Based on the β decay of ^{59}Fe [12].
[c]Assumption based on the empirical distribution of $\log ft$ [21].

the B(GT) strengths for the allowed transitions from the ^{59}Co ground state to the ^{59}Fe excited states were derived [19,20]. The B(GT) values of these transitions are listed in Table I, along with ground state β decay. Due to the limit of energy resolution ($\sigma \sim 0.9$ MeV), the extracted B(GT) value has a large uncertainty of $\sim$40%.

We have done shell model calculations with GXPF1a and GXPF1j interactions to evaluate the GT transitions between the $7/2^-$ ground state and $3/2^-$ low-lying states in ^{59}Co and the states in ^{59}Fe. Several calculations have been done by restricting the maximal number of particles (denoted as $N_{\max}$) that can be excited from the $f_{7/2}$ orbital to the other orbitals above the $N = Z = 28$ shell closures. It is seen that calculations for the low-lying states with $N_{\max} = 6$ have basically converged and are nearly identical with those calculated in the full model space. We have taken $N_{\max} = 6$ for our calculations of higher lying states. We have calculated the lowest 100 states for each spin by using the Lanczos approach. The B(GT) values of low-lying states of ^{59}Fe to ^{59}Co are listed in Table II. The B(GT) for ^{59}Fe $(5/2^-,$ 472 keV) → ^{59}Co $(7/2^-$ g.s.) is calculated to be 9.33×10^{-3} and 9.87×10^{-3} with the quenching factor 0.79^2 of B(GT) for GXPF1a and GXPF1j, respectively. Both results are about 1/3 of the experimental values.

Besides decaying to the ground state of ^{59}Co, the states of ^{59}Fe shown in Fig. 1 can also decay to the excited states

TABLE II. Summary of the shell model B(GT) values for the allowed transitions from low-lying states of ^{59}Fe to ^{59}Co. A quenching factor of 0.79^2 has been applied to the B(GT) values.

Transitions	GXPF1a	GXPF1j
472 keV → g.s.	9.33×10^{-3}	9.87×10^{-3}
1023 keV → g.s.	2.88×10^{-6}	4.42×10^{-5}
281 keV → 1099 keV	6.44×10^{-2}	3.54×10^{-2}
281 keV → 1292 keV	2.00×10^{-2}	3.92×10^{-2}
472 keV → 1099 keV	2.33×10^{-3}	2.20×10^{-3}
472 keV → 1292 keV	2.00×10^{-4}	1.33×10^{-4}
571 keV → 1099 keV	1.03×10^{-1}	1.00×10^{-1}
571 keV → 1292 keV	3.00×10^{-3}	1.30×10^{-3}
726 keV → 1099 keV	2.12×10^{-2}	1.62×10^{-2}
726 keV → 1292 keV	2.60×10^{-2}	2.85×10^{-2}

of ^{59}Co, e.g., 1099 keV ($3/2^-$) and 1292 keV ($3/2^-$), with allowed transitions. The measurement of the β decay of ^{59}Fe provides the B(GT) strengths from the ground state of ^{59}Fe to the two excited states. However, other transitions from the excited states of ^{59}Fe to the excited states of ^{59}Co are not accessible for the charge exchange reaction. We choose to use empirical $\log ft = 5.9$ based on β-decay statistics with a selection-rule [22] for other allowed transitions to ^{59}Co excited states, which are also listed in Table I. The same procedure was also employed in FFN weak interaction rates [6] while the results of Ref. [22] are based on a more recent nuclear database. It is worthwhile to mention that the B(GT) values listed in Tabel II agree with the empirical $\log ft = 5.9 \pm 1.0$ (1σ) [$4.87 \times 10^{-4} < B$(GT)$ < 4.87 \times 10^{-2}$] except for the weak transition 1023 keV $\rightarrow$ g.s. (9.1 for GXPF1a and 7.9 for GXPF1j) and strong transition 571 keV $\rightarrow$ 1292 keV (4.6 for GXPF1a and GXPF1j). However, these two transitions are a minor contribution in ^{59}Fe due to the weakly thermal population (1023 keV $\rightarrow$ g.s.) and small decay phase space (571 keV $\rightarrow$ 1292 keV).

B. ^{59}Fe β-decay rate at stellar temperature

The partial half-life of the ith state of ^{59}Fe to ^{59}Co can be obtained with

$$\frac{1}{t_i} = \sum_j 10^{-(\log ft_{ij} - \log f)},$$

$$\frac{1}{ft_{ij}} = \frac{K}{\lambda^2} B(\text{GT})_{ij}.$$

Here, $K = 6146$ s, $\lambda^2 = (1.2599)^2$ [21], and f is the phase space integral. The half-life of ^{59}Fe in the stellar environment is given by Eq. (2).

The rates obtained from the experimental and empirical B(GT) values in Table I and shell-model B(GT) values in Table II are shown in Fig. 3(a). The density of hydrostatic and explosive burning relevant to ^{60}Fe nucleosynthesis is below 10^5 g/cm^3, at which the rate is insensitive to the density. At low temperature ($T < 0.5$ GK) the g.s. β decay dominates the rate. Therefore, for He-shell burning, there is no difference between these sets of rates. With raising temperature, the decay rate increases rapidly. At $T = 1.2$ GK, which is a typical C-shell burning temperature, our stellar rate is about two orders of magnitude higher than the ground state decay rate (1.80×10^{-7} s^{-1}). The rates based on shell model calculation with variants of the GXPF1 interaction are closer to the one derived from experimental data than FFN and LMP rates, which show one order of magnitude difference. This indicates the capability of GXPF1a and GXPF1j interactions in describing GT strengths of $A \sim 60$ nuclei.

C. Uncertainties for the ^{59}Fe β-decay rate

The uncertainty of our ^{59}Fe decay rate comes from several aspects: experimental uncertainties of B(GT) strengths obtained from charge exchange reaction, empirical $\log ft$ values for the unmeasured transitions, cutoff in excited states, and the
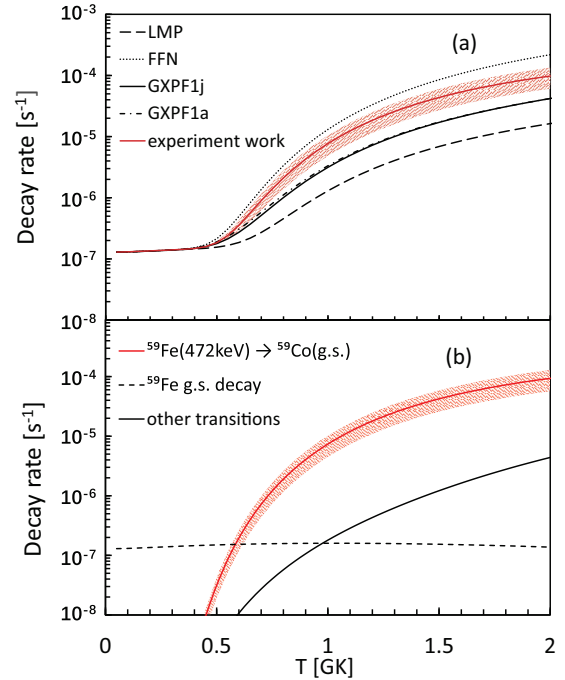

FIG. 3. (a) The stellar β-decay rate of ^{59}Fe as a function of temperature. The shaded area represents the uncertainty incurred by the experimental B(GT) values. FFN and LMP rates are plotted with dotted and dashed lines, respectively. Shell model calculations based on GXPF1a and GXPF1j interactions are also plotted with solid and dash-dotted lines. (b) The β-decay rates contributed by various transitions of ^{59}Fe $\rightarrow$ ^{59}Co as a function of temperature. The red line represents the dominant transition ^{59}Fe (472 keV) $\rightarrow$ ^{59}Co (g.s.), while the shaded area represents the uncertainty due to the experimental B(GT) error. The ground state decay and other allowed transitions are presented with dashed and solid lines, respectively.

dubious states. In this section, we discuss their contributions to the uncertainty of the ^{59}Fe β-decay rate.

The stellar decay rate of ^{59}Fe is dominated by the transitions from the ^{59}Fe ground state decay and by the allowed transitions from ^{59}Fe excited states to the ^{59}Co ground state [e.g., ^{59}Fe(472 keV) $\rightarrow$ ^{59}Co(g.s.)] in the range $T < 2$ GK. The contributions from different transitions to the ^{59}Fe β-decay rate are illustrated in Fig. 3(b) as a function of temperature. One can see that the transition ^{59}Fe(472 keV) $\rightarrow$ ^{59}Co(g.s.) dominates the total decay rate in the region $0.5 < T < 2.0$ GK. Other allowed transitions contribute less than 10%.

To emphasize the importance of the ^{59}Fe(472 keV) $\rightarrow$ ^{59}Co(g.s.) transition, we also calculated the decay rate which only takes this transition and ground state decay into account by setting the $\log ft$ of all other transitions to be infinity. The deviation is less than 4% at $T < 2.0$ GK. It indicates that this transition plays an important role in the stellar β decay. The large error bar associated with the transition strength results in about 40% uncertainty in the decay rate at the typical C-shell burning temperature $T = 1.2$ GK.

The uncertainty incurred by the usage of empirical $\log ft$ for the unmeasured transitions has been investigated by varying the $\log ft$ values within a range obtained from observation.
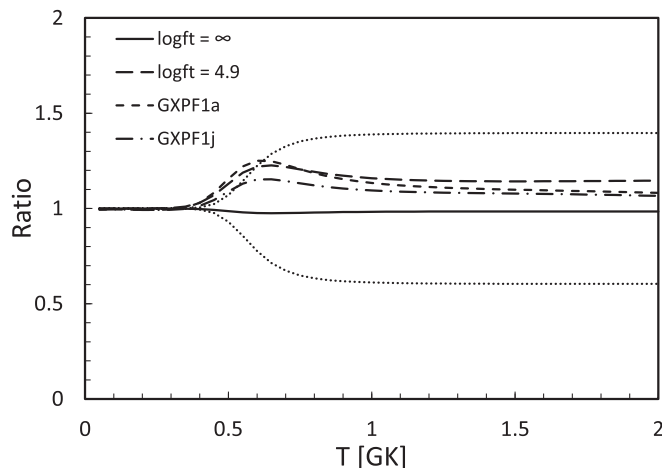
FIG. 4. The impact on ^{59}Fe stellar β-decay rate from various uncertainties. Dotted lines represent the uncertainty due to the experiment data error of B(GT). The rates with empirical $\log ft = 4.9$ and $\log ft = $ infinity are presented with dashed and solid lines, respectively. Shell model calculations with GXPF1a and GXPF1j interactions for other transitions are plotted with short-dashed and dash-dotted lines, respectively.
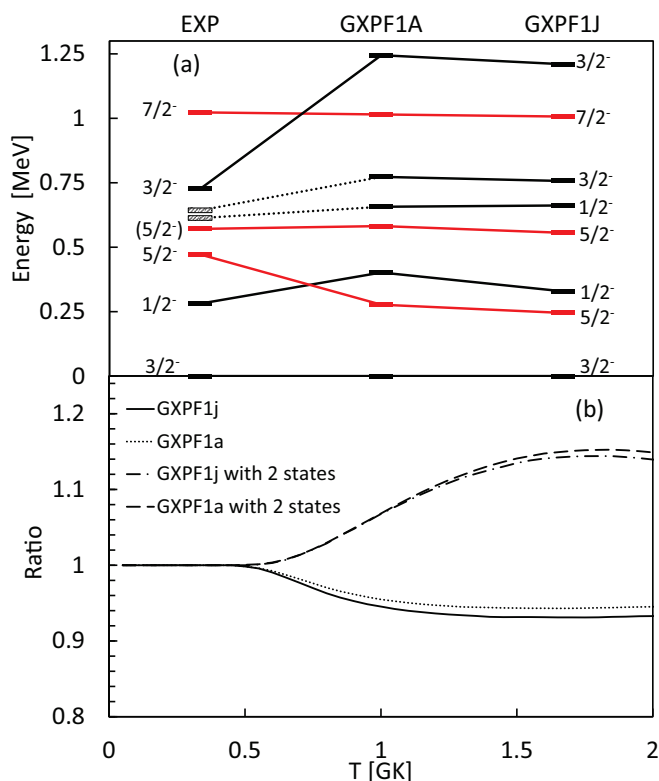

FIG. 5. (a) The alternative mapping of the shell model calculation with 571 keV assigned to $5/2^-$. The mappings with two dubious sates (613 and 643 keV) are shown with dotted lines. (b) The relative decay rates with alternative assignment of shell model energy levels of ^{59}Fe. Shell model calculations with 571 keV assigned to $5/2^-$ for GXPF1a and GXPF1j interactions, and with two additional dubious states for GXPF1a and GXPF1j interactions, are plotted with dotted, solid, dash-dotted and dashed lines, respectively.

According to the β-decay statistics, the $\log ft$ for allowed transitions is distributed in the range 4.9 to 6.9 ($\pm 1\sigma$) [22]. The decay rate with $\log ft = 4.9$ is shown in Fig. 4 with a dashed line. At temperature $T = 1.2$ GK, the decay rate increases about 15% with $\log ft = 4.9$, which is less than the 40% uncertainty incurred by the experimental B(GT) values for the transition ^{59}Fe(472 keV) $\rightarrow$ ^{59}Co(g.s.). The solid line by setting $\log ft$ to infinity can serve as the lower limit for the contributions to the total decay rate. The calculations with variants of the GXPF1 interaction for other allowed transitions are also presented in Fig. 4. One can see the rates based on these two interactions are still within the uncertainty incurred by the experimental error of the B(GT) of ^{59}Fe(472 keV) $\rightarrow$ ^{59}Co(g.s.).

To investigate the contribution of the higher-lying states, we recalculate the decay rate by including the excited states of ^{59}Fe up to 2 MeV and the excited states of ^{59}Co up to 1.5 MeV. In the calculation, both allowed and first-forbidden transitions are included. Empirical $\log ft$ values from Ref. [22] are used for unmeasured transitions up to 2 MeV states. The result only increases 1% when $T < 2$ GK. For higher temperature, such as the explosive burning scenario, we will show in the next section that the decay rate is not so critical as it is at C-shell burning temperature. Thus, the decays of ^{59}Fe states higher than 1 MeV can be ignored for ^{60}Fe nucleosynthesis. Such a conclusion is also confirmed by the shell model calculations, which include excited states up to 10 MeV.

The ^{59}Fe(571 keV) state is preferred to be $3/2^-$ in the present work according to Ref. [14], thus the assignments of energy level of the shell model calculation have been made as shown in Fig. 2. We have also done calculations with alternative assignments in which the ^{59}Fe(571 keV) state was assigned as $5/2^-$, thus undergoing an allowed transition to the ^{59}Co ground state as shown in Fig. 5(a). The B(GT)

strength for the transition of this state to ^{59}Co(g.s.) is taken to be 8.3×10^{-4} for GXPF1a and 1.2×10^{-3} for GXPF1j as the predicted strength of the unmapped $5/2^-$ by shell model calculation. A comparison of the rates based on these two different spin assignments is plotted in Fig. 5(b). One can see that the rates with the two different assignments have less than 10% difference. This is mainly due to the relatively small B(GT) of ^{59}Fe (571 keV) $\rightarrow$ ^{59}Co (g.s.) in the shell model calculation, leading to lower contribution than that of ^{59}Fe (472 keV) $\rightarrow$ ^{59}Co (g.s.). Future high resolution charge exchange measurements could help to resolve this ambiguity.

The $E_x = 613$ keV and 643 keV states are excluded in the present work due to lack of enough information. However, we performed the shell model calculation with the two dubious states with the mapping presented in Fig. 5(a). The relative decay rates are plotted in Fig. 5(b). After adding these two states, the decay rates are about 15% higher. The uncertainty in relation to their contribution to the stellar decay rate can also be reduced with the charge exchange experiment.

It is clear that the uncertainty of the B(GT) value of ^{59}Fe(472 keV) $\rightarrow$ ^{59}Co(g.s.) is the dominant source in the error budget. Therefore, the determination of the transition strength of this allowed transition to the ^{59}Co ground state
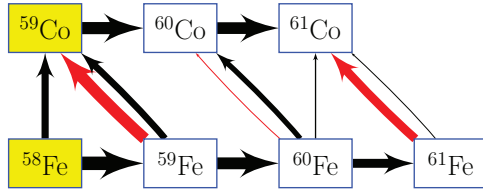
FIG. 6. Net current chart of ^{60}Fe nucleosynthesis in C-shell burning. The red lines present β decay, while the black lines present the nuclear reactions such as (n,γ) and (p,n). Line width indicates the flow current in logarithmic scale.

will be essential for determining the ^{59}Fe stellar β-decay rate at the C-shell burning temperature. This can be done with a ^{59}Co$(t,^3$He$)^{59}$Fe or ^{59}Co$(d,^2$He$)^{59}$Fe experiment with higher resolution.

IV. IMPACT ON THE ^{60}Fe NUCLEOSYNTHESIS

^{60}Fe are mainly synthesized in He-shell burning and C-shell burning together with explosive C/Ne burning [1]. The temperature of He-shell burning is $\sim$0.4 GK, where the ^{59}Fe β decay is still dominated by the ground state decay; see, e.g., Fig 3. However, the temperature of C-shell burning and explosive burning is higher than 1 GK, thus the impact on the nucleosynthesis of ^{60}Fe with the ^{59}Fe stellar β-decay rate should be investigated.

A. Carbon-shell burning

We employ the network calculation code NUCNET [23], to calculate the nucleosynthesis of ^{60}Fe. In the original NUCNET code the terrestrial β-decay rate was used for the calculation. The trajectory of temperature and density for the C-shell burning processes and initial abundances are taken from Ref. [24]. The temperature and density of C-shell burning are $\sim$1.2 GK and 1×10^5 g/cm^3, respectively. The net current chart for ^{60}Fe production in the C-shell burning phase is shown in Fig. 6, which is generated by NUCNET code. One can see that the β decay of ^{59}Fe competes with its neutron capture reaction, which would affect the synthesis of ^{60}Fe. The abundance of ^{60}Fe produced by C-shell burning has been calculated with six different ^{59}Fe decay rates: terrestrial rate, FFN rate, LMP rate, and our rates based on GXPF1a, GXPF1j, and experiment data. The results are shown in Fig. 7. With our rate based on experimental work, the abundance of ^{60}Fe drops to 30% compared with the one obtained from the terrestrial rate. The abundance uncertainty of ^{60}Fe incurred by the ^{59}Fe decay rate is about 30%. It shows the importance of the ^{59}Fe stellar β-decay rate to the ^{60}Fe synthesis in th C-shell burning scenario. The abundance obtained from LMP is three times larger than the one obtained from FFN rate. With the new ^{59}Fe rate, the predicted ^{60}Fe/^{26}Al decay flux ratio is expected to be lower than the current prediction [5] based on the LMP rate. Therefore, it is helpful to resolve the existing discrepancy between the theory and observation.

Besides β decay, the ^{59}Fe(n,γ) rate also plays an important role in ^{60}Fe synthesis. In the present work the (n,γ) rate is taken from REACLIB [25] based on theoretical calculation.
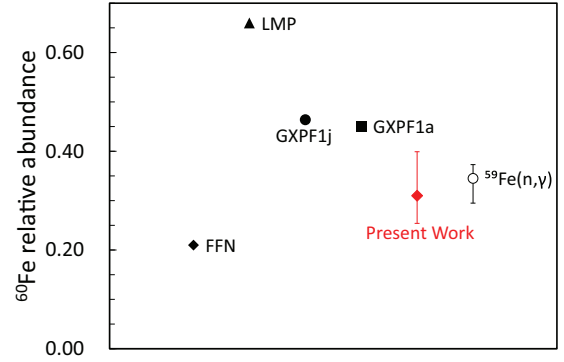

FIG. 7. Relative ^{60}Fe abundances in the C-shell burning scenario calculated respectively with terrestrial rate, FFN rate, LMP rate, GXPF1a rate, GXPF1j rate, and our rate for ^{59}Fe β decay. The results have been normalized by the ^{60}Fe abundances obtained with the terrestrial ^{59}Fe rate. The ^{60}Fe abundance obtained with our rate based on charge exchange data is shown as a red diamond. The ^{60}Fe abundance uncertainty incurred by ^{59}Fe(n,γ) is shown for comparison.

Recent experimental data is available based on ^{60}Fe(γ,n) measurement [26]. The new rate is $\sim$20% higher than the REACLIB rate. We update the ^{59}Fe$(n,\gamma)^{60}$Fe reaction rate and repeat the C-shell burning calculation. Results are shown in Fig. 7. The abundance uncertainty of ^{60}Fe incurred by ^{59}Fe$(n,\gamma)^{60}$Fe is about 20%, less than the one incurred by the ^{59}Fe stellar decay rate.

B. Explosive burning

Explosive C/Ne burning would also contribute a certain amount of ^{60}Fe [1]. The current chart for explosive burning is shown in Fig. 8. The trajectory of temperature and density for the C-shell burning processes and initial abundances are based on a $20M_{sun}$ model taken from Ref. [1]. The peak temperature and density of explosive burning are $\sim$2.3 GK and 3.2×10^5 g/cm^3. With the high temperature and density, (p,n) dominates while β decay is just a minor part of the ^{59}Fe destruction channel. This is mainly due to the fact that the latter is not as sensitive to temperature and density as the former. Our calculations show that the ^{60}Fe abundance calculated with various β-decay rates gives less than 10^{-3} difference in the explosive burning. But one needs keep in mind that the ^{60}Fe from the explosive burning shell has a significant fraction produced by the preceding C-shell burning
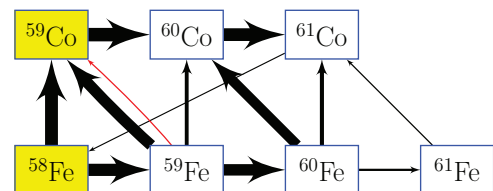

FIG. 8. Net current chart of ^{60}Fe nucleosynthesis in explosive burning.

before the explosion. Therefore, it is important to obtain a reliable ^{59}Fe decay rate at C-shell burning temperature.

V. SUMMARY

We have utilized the charge exchange experimental data to determine the GT transition strength from ^{59}Fe low-lying states to the ^{59}Co ground state and to obtain a new stellar β-decay rate of ^{59}Fe. The new ^{59}Fe β-decay rate is up to a factor of 2.5 lower than FFN rate and up to a factor of 5 higher than LMP rate in the temperature range $0.5 \leqslant T \leqslant 2$ GK. The new rate agrees well with those derived from our large-scale shell model calculations. Our analysis indicates that at carbon-shell burning temperature the transition of the excited state $E_x = 472$ keV of ^{59}Fe to the ground state of ^{59}Co is essential for the ^{59}Fe stellar β-decay rate. Its contribution is one order of magnitude higher than those from other transitions. Due to the limitations of (n, p) measurement, the insufficient experiment resolution ($\sigma \sim 0.9$ MeV) leads a large uncertainty in the ^{59}Fe stellar β-decay rate. The impact on ^{60}Fe synthesis with stellar β-decay rate is studied with a one-zone model calculation. It shows that ^{59}Fe stellar β decay would significantly affect the ^{60}Fe synthesis in the carbon shell burning scenario. With the new ^{59}Fe decay rate, the predicted ^{60}Fe/^{26}Al decay flux ratio is expected to be lower than the current prediction [5]. It will help to resolve the existing discrepancy between the theory and observation. To reduce the uncertainty arising from the ^{59}Fe stellar decay rate, one may expect that further investigations of reactions such as $(t, {}^3\text{He})$ and $(d, {}^2\text{He})$ would not only help

to confirm the spin-parity assignment for the low-lying states of ^{59}Fe, but also to obtain more precise transition strengths to reduce the uncertainty in ^{60}Fe nucleosynthesis.

[1] M. Limongi and A. Chieffi, Astrophys. J. **647**, 483 (2006).

[2] W. Wang *et al.*, Astron. Astrophys. **469**, 1005 (2007).

[3] D. Smith, in *Proceedings of the 5th INTEGRAL Workshop: The INTEGRAL Universe, February 2004, Munich*, edited by D. Battrick, ESA Special Publication No. 552 (European Space Agency, Paris, 2005), p. 45.

[4] F. X. Timmes *et al.*, Astrophys. J. **449**, 204 (1995).

[5] S. E. Woosley and A. Heger, Phys. Rep. **442**, 269 (2007).

[6] G. M. Fuller, W. A. Fowler, and N. J. Newman, Astrophys. J. **252**, 715 (1982).

[7] P. M. Endt and C. Van Der Leun, Nucl. Phys. A **310**, 1 (1978).

[8] K. Takahashi and K. Yokoi, At. Data Nucl. Data Tables **36**, 375 (1987).

[9] K. Langanke and G. Martinez-Pinedo, At. Data Nucl. Data Tables **79**, 1 (2001).

[10] E. Caurier *et al.*, Nucl. Phys. **653**, 439 (1999).

[11] A. L. Cole, T. S. Anderson, R. G. T. Zegers, S. M. Austin, B. A. Brown, L. Valdez, S. Gupta, G. W. Hitt, and O. Fawwaz, Phys. Rev. C **86**, 015809 (2012).

[12] NNDC data base, http://www.nndc.bnl.gov.

[13] E. K. Warburton, J. W. Olness, A. M. Nathan, J. J. Kolata, and J. B. McGrory, Phys. Rev. C **16**, 1027 (1977).

[14] K. C. McLean *et al.*, Nucl. Phys. A **191**, 417 (1972).

[15] R. Vennink *et al.*, Nucl. Phys. A **344**, 421 (1980).

[16] J. H. Bjerregaard *et al.*, Nucl. Phys. **51**, 641 (1964).

[17] M. Honma, T. Otsuka, B. A. Brown, and T. Mizusaki, Eur. Phys. J. A **25** Suppl. 1, 499 (2005).

[18] M. Honma *et al.*, J. Phys.: Conf. Ser. **20**, 7 (2005).

[19] M. B. Aufderheide, S. D. Bloom, D. A. Resler, and G. J. Mathews, Phys. Rev. C **47**, 2961 (1993).

[20] W. P. Alford, B. A. Brown, S. Burzynski, A. Celler, D. Frekers, R. Helmer, R. Henderson, K. P. Jackson, K. Lee, A. Rahav, A. Trudel, and M. C. Vetterli, Phys. Rev. C **48**, 2818 (1993).

[21] I. S. Towner and J. C. Hardy, in *Symmetries and Fundamental Interactions in Nuclei*, edited by W. C. Haxton and E. M. Henley (World Scientific, Singapore, 1995) p.183.

[22] B. Singh *et al.*, Nucl. Data Sheets **84**, 487 (1998).

[23] M. J. Bojazi and B. S. Meyer, Phys. Rev. C **89**, 025807 (2014).

[24] M. Pignatari *et al.*, Astrophys. J. **762**, 31 (2013).

[25] R. H. Cyburt *et al.*, Astrophys. J. **189**, 240 (2010).

[26] E. Uberseder, T. Adachi, T. Aumann, S. Beceiro-Novo, K. Boretzky, C. Caesar, I. Dillmann, O. Ershova, A. Estrade, F. Farinon, J. Hagdahl, T. Heftrich, M. Heil, M. Heine, M. Holl, A. Ignatov, H. T. Johansson, N. Kalantar, C. Langer, T. LeBleis, Y. A. Litvinov, J. Marganiec, A. Movsesyan, M. A. Najafi, T. Nilsson, C. Nociforo, V. Panin, S. Pietri, R. Plag, A. Prochazka, G. Rastrepina, R. Reifarth, V. Ricciardi, C. Rigollet, D. M. Rossi, D. Savran, H. Simon, K. Sonnabend, B. Streicher, S. Terashima, R. Thies, Y. Togano, V. Volkov, F. Wamers, H. Weick, M. Weigand, M. Wiescher, C. Wimmer, N. Winckler, and P. J. Woods, Phys. Rev. Lett. **112**, 211101 (2014).